# CONFIDENCE REGIONS ON SEISMIC EVENT LOCATIONS BASED ON MULTIPLE-EVENT ANALYSIS

William L. Rodi and M. Nafi Toksöz

Massachusetts Institute of Technology

Sponsored by Defense Threat Reduction Agency

Contract No. DTRA01-00-C-0102

## ABSTRACT

We have developed a new approach to analyzing seismic event location uncertainty. The approach is based on a maximum-likelihood statistical framework and implemented with numerical techniques such as grid search and Monte Carlo simulation. It determines confidence regions on event locations under a general class of picking error models (Gaussian and non-Gaussian) and taking the nonlinear dependence of travel-time on event location into account. Non-Gaussian error distributions and nonlinear analysis lead to confidence regions that depart significantly from the elliptically shaped confidence regions obtained with the conventional Gaussian/linear approach, especially in the case of sparsely recorded events. Our recent focus has been on how errors in travel-time tables ("modeling" errors) affect event location uncertainty. Such errors are usually accommodated through an augmentation of the error model assumed in the uncertainty analysis, using an appropriate probability distribution for modeling errors determined from the analysis of calibration data from ground-truth (GT) events. This conventional approach, however, presents severe difficulties such as accounting for errors in GT event locations and parameterizing the dependence of the modeling error distribution on event location. We have adopted an alternative approach in which location uncertainty is analyzed in conjunction with a calibration analysis, i.e. performing the uncertainty analysis in the context of the multiple-event location problem in which the location parameters of a set of events are determined jointly with travel-time corrections associated with the paths between the events and recording stations. Uncertainty analysis in this joint inverse problem considers the trade-offs between location parameters and travel-time corrections, and thus the location confidence regions inferred for individual events implicitly account for the effect of calibration uncertainty (errors in path corrections). We have implemented this approach on the small-cluster multiple-event location problem, where path corrections are assumed to be station-dependent but event-independent, by extending our grid search/Monte Carlo algorithm for single-event location. We are testing our new approach to location uncertainty on regional and teleseismic arrival time data from the 1999 Izmit and Duzce earthquake clusters.

## OBJECTIVE

The objective of this work is to develop a methodology for seismic event location that provides reliable estimates of location uncertainty needed in nuclear event monitoring. In previous work (Rodi and Toksöz, 2000, 2001) we have formulated a theoretical approach to event location uncertainty in terms of likelihood functions and hypothesis testing and implemented the approach with grid-search and Monte Carlo techniques. The resulting algorithm computes confidence regions on event locations that account for such complexities as nonlinearity of the forward travel-time problem and non-Gaussian distributions of observational (picking) errors. A major objective of our project has been to also incorporate a rigorous treatment of the errors in travel-time models (modeling errors) into our uncertainty analysis. Toward this goal, we have linked our uncertainty analysis to the process of seismic travel-time calibration, recognizing that modeling errors are due to the uncertainty in calibration parameters such as path corrections and tomographic velocity models. Therefore, we have extended our formulation to the multiple-event location problem, i.e., whereby data from multiple events and stations are used to simultaneously infer the locations of the events and calibration parameters. The trade-offs and correlations among the unknowns of this joint inverse problem affect an implicit account of modeling errors. Our first step in implementing this formulation was to extend our single-event grid-search location algorithm (known as GSEL) to a multiple-event one (GMEL). Currently, GMEL only solves the basic multiple-event location problem, applicable to event clusters of small spatial aperture, in which calibration parameters comprise an event-independent travel-time correction for each station. This algorithm is described in Rodi et al. (2002), where it is also compared to some other multiple-event location algorithms. In the present paper, we describe our formulation of multiple-event location uncertainty and our efforts to implement it in an extended version of GMEL.

## RESEARCH ACCOMPLISHED

### Formulation

We state our formulation of the joint location/calibration inverse problem for the special case of a data set comprising only seismic arrival times, with at most one seismic phase observed for each event-station pair. If there are $m$ seismic events ($i = 1, \ldots, m$) and $n$ seismic stations ($j = 1, \ldots, n$), the inverse problem can be written as

$$d_{ij} = t_i + T_j(\mathbf{x}_i) + c_{ij} + e_{ij} \qquad (1)$$

where $d_{ij}$ is the observed arrival time for the $(i,j)$th path; $t_i$ and $\mathbf{x}_i$ are origin parameters (time and hypocenter, respectively) of the $i$th event; $T_j$ is a model-based travel-time function for the $j$th station; $c_{ij}$ is a correction to this function; and $e_{ij}$ is an observational error in $d_{ij}$. This equation holds for the station/event pairs for which data have been observed. The unknown parameters of this joint calibration/location inverse problem are the event hypocenters and origin times ($\mathbf{x}_i$ $t_i$, $i = 1, \ldots, m$) and the path correction $c_{ij}$.

The exact nature of the inverse problem depends on how the path corrections $c_{ij}$ are parameterized, and what prior constraints are imposed on them and the event origin parameters. On the latter issue, the problem is purely one of calibration when the event parameters are assumed known, and purely one of location when the path corrections are known. In practice, neither set of parameters is completely known or unknown. Two difficult problems in nuclear discrimination, in fact, are the same problem in this formulation. The first is how to account for uncertainty in a seismic calibration (errors in estimates of $c_{ij}$) when the calibration events have imperfectly known locations, i.e. ground-truth (GT) levels greater than 0. The second, which is the focus of this project, is how the location error of any particular event is affected by imperfect knowledge of the path corrections. These are two aspects of a complete uncertainty analysis in the joint calibration/location problem.

### Parameterization of Path Corrections

The multiple-event inverse problem is hopelessly ill posed if the path corrections are not constrained via prior information or a parameterization that reduces the number of independent unknowns, or both. In the basic multiple-event location problem, relevant to small event clusters, the path corrections are assumed to be event-independent, i.e.

$$c_{ij} = a_j. \qquad (2)$$

The calibration parameters comprise a time term, $a_j$, for each station. Our work on uncertainty analysis to date has focused on this basic problem. However, our formulation pertains to other ways of parameterizing path corrections, such as with correction functions (or surfaces):

$$c_{ij} = a_j(\mathbf{x}_i). \tag{3}$$

Here, there is an unknown function, $a_j(\mathbf{x})$ assigned to each station. It also pertains to the universal parameter functions described by Rodi et al. (2003). When spatial functions are used to parameterize travel-time corrections, however, it is necessary to provide additional prior information on their smoothness, such as with geo-statistical constraints (e.g. Schultz et al., 1998).

**Maximum-Likelihood Formulation**

Our approach to inverse problems and uncertainty analysis is based on likelihood functions. A likelihood function is a function of the unknown parameters whose purpose is to quantify how well any given values for the parameters agree with the observed data. An optimal estimate of the unknown parameters is taken to be those values that maximize the likelihood function (the *maximum-likelihood* estimate). A confidence region on the parameters is the collection of parameter values whose likelihood is within some tolerance of the maximum likelihood.

A given assumption about the probability distribution of the data errors defines a particular likelihood function for the parameters. In our location algorithms GSEL and GMEL, we currently assume that the picking errors, $e_{ij}$, are statistically independent and that each has a *generalized Gaussian* probability distribution of order $p$. The probability density function (p.d.f.) of this distribution is given by (Billings et al., 1994)

$$f[e_{ij}] = \frac{\text{const}}{\sigma_{ij}} \exp\left[-\frac{1}{p}\left|\frac{e_{ij}}{\sigma_{ij}}\right|^p\right] \tag{4}$$

where $\sigma_{ij}$ is the assigned standard error. For $p = 1$, the p.d.f. is a Laplace distribution (two-sided exponential) and for $p = 2$ it is Gaussian. For the small-cluster problem ($c_{ij} = a_j$), this error model implies a likelihood function, $L$, given by

$$-\log L = \text{const} + \sum_{ij} \log\sigma_{ij} + \frac{1}{p}\sum_{ij}\frac{1}{(\sigma_{ij})^p}\left|d_{ij} - t_i - T_j(\mathbf{x}_i) - a_j\right|^p. \tag{5}$$

We comment that, with the generalized Gaussian distribution, the negative logarithm of the likelihood function is an $L_p$ norm (to the $p$th power) of the data residuals. In the Gaussian case it is an $L_2$ norm, and maximization of the likelihood function with respect to the problem unknowns becomes a least-squares problem.

When correction functions, instead of correction terms, are used to parameterize path corrections, an additional term can be added to $L$ in order to invoke geo-statistical constraints (see Rodi et al., 2003).

**Single-Event Confidence Regions**

We briefly describe our uncertainty approach to location error in the single-event location problem and refer the reader to Rodi and Toksöz (2001) for further detail. To define the single-event problem in our notation we can drop the event index $i$ in equation (1). To simplify this discussion, let us also set path corrections to zero, yielding

$$d_j = t + T_j(\mathbf{x}) + e_j. \tag{6}$$

Our current single-event algorithm (GSEL) assumes that the data standard errors are known within a constant factor, i.e.

$$\sigma_j = \sigma\sigma_j \tag{7}$$

with the $w_j$ being known weights and with $\sigma$ the unknown standard error across all the data. The problem unknowns are then the event parameters, **x** and *t*, and $\sigma$. The log likelihood function from equation (5) becomes

$$-\log L(\mathbf{x}, t, \sigma; \mathbf{d}) = \text{const} + n \log \sigma + \frac{1}{p\sigma^p} \sum_i \frac{1}{(w_j)^p} \left| d_j - t - T_j(\mathbf{x}) \right|^p . \qquad (8)$$

Here, **d** denotes the arrival time data ($d_j$) collectively as an *n*-component vector.

Our single-event location algorithm uses a grid-search technique to maximize *L* with respect to the event hypocenter **x**. For each hypocenter in a 3-D grid, the algorithm computes a reduced likelihood function, i.e. maximized with respect to *t* and $\sigma$ with **x** fixed. The maximization over $\sigma$ and *t* is performed with analytic and root-finding techniques. The hypocenter grid is constructed dynamically through a process of successive refinement, along the lines of Sambridge's (1999) neighborhood algorithm. The search finds the hypocenter that yields the largest reduced likelihood among all grid nodes tested. To incorporate hard bounds on the event hypocenter (GT constraints), one simply eliminates grid nodes violating the bounds from the search.

Flinn (1965), Evernden (1969) and Jordan and Sverdrup (1981) developed the methodology for hypocentral confidence regions for the case of Gaussian data errors ($p = 2$) and using a linear approximation to the travel-time functions, $T_j$. Their methods can be formulated in terms of hypothesis testing using a likelihood ratio as the test statistic. Doing so allows us to define confidence regions under less restrictive assumptions.

Confidence regions can be found on all four location parameters simultaneously (including origin time) or on any subset of parameters. For a 3-D, hypocentral confidence region on **x**, the relevant test statistic is

$$\Lambda(\mathbf{x}, \mathbf{d}) = \log \left[ \frac{\max_{x,t,\sigma} L(\mathbf{x}, t, \sigma; \mathbf{d})}{\max_{t,\sigma} L(\mathbf{x}, t, \sigma; \mathbf{d})} \right]. \qquad (9)$$

This statistic compares the value of *L* achieved by maximizing it over all unknown parameters to the value of *L* when maximized over only *t* and $\sigma$, with the hypocenter fixed to any given **x**. Given a confidence level $\alpha$, we can reject **x** at that level if $\Lambda(\mathbf{x},\mathbf{d})$ is greater than some critical value, $\Lambda_\alpha$. This critical value is determined by the probability distribution of $\Lambda(\mathbf{x},\mathbf{d})$, as induced by the errors in **d**. If **x** is *not* rejected, it is *inside* the confidence region for the specified confidence level. That is, the confidence region comprises the hypocenters **x** satisfying

$$\Lambda(\mathbf{x},\mathbf{d}) \le \Lambda_\alpha . \qquad (10)$$

Under Flinn's assumptions, $\Lambda$ is F-distributed and $\Lambda_\alpha$ can be found directly from the F cumulative distribution function (c.d.f.). The locus of points **x** satisfying equation (10) fills an ellipsoid whose axis lengths and orientations are easily found.

With our more general assumptions, $\Lambda$ does not necessarily have a well-known probability distribution and the geometry of the confidence region cannot be found with analytic formulas. Therefore, we use numerical techniques to find $\Lambda_\alpha$ and the values of **x** that satisfy equation (10). Our confidence region method becomes a two-step procedure:

1. Sample $\Lambda(\mathbf{x},\mathbf{d})$ at points **x** on a dense 3-D hypocenter grid. This entails maximizing *L* with respect to origin time and $\sigma$ for each point on the grid, and comparing each such value to the maximum *L* over all parameters (i.e. the maximum likelihood solution).

2. Perform a Monte Carlo simulation to find $\Lambda_\alpha$ for various $\alpha$. This entails computing $\Lambda(\mathbf{x}^{\text{tru}},\mathbf{d}^{\text{syn}})$ for an assumed "true" hypocenter $\mathbf{x}^{\text{tru}}$ and many realizations of synthetic data, $\mathbf{d}^{\text{syn}}$. Each realization $\mathbf{d}^{\text{syn}}$ is constructed by adding a realization of pseudo-random errors to arrival times calculated for $\mathbf{x}^{\text{tru}}$. The random noise is generated according to the assumed error distribution using an assumed "true" value of $\sigma$.

Both steps of this procedure can be computationally intensive. The first step (likelihood sampling) requires maximizing $L$ for all hypocenters on a 3-D grid, but only for the real data. The second step (Monte Carlo simulation) entails maximizing $L$ twice, with $\mathbf{x}$ fixed and free, for each of many realizations of synthetic data. We have found that about 200–300 realizations of synthetic data yield stable results.

Confidence regions on other event parameters are obtained in an analogous manner, and share some of the calculations needed for hypocentral regions. For epicenter confidence regions, for example, one changes the likelihood-ratio statistic in equation (9) to include maximization with respect to event depth, $z$, in addition to $t$ and $\square$.

**Examples**

An example of our approach, which demonstrates the importance of accounting for travel-time nonlinearity, is shown in Figure 1. This figure displays confidence regions for an earthquake in Honshu, Japan, as determined from mostly first-arrival, teleseismic data obtained by the International Monitoring System (IMS) seismic network. Each figure shows the 2-D confidence region of the event epicenter (at varying confidence levels) and cross-sections through the 3-D confidence region on the event hypocenter. The IASP91 travel-time tables were used in these computations, and the best-fitting location of the event is in the mantle of the IASP91 model (depth = 44 km). The epicenter confidence region for each confidence level (right of figure) is nearly elliptical in shape. The corresponding hypocentral confidence region, however, is quite non-ellipsoidal and extends upward into the crust (left and middle frames). This is an effect of nonlinearity that is not accounted for with the conventional Gaussian/linear formulas. The cause of it is the velocity difference, and consequent difference in the sensitivity of travel-time to event depth ($dT/dz$), across the Moho. The conventional confidence ellipsoid formulas in this case would assume the mantle $dT/dz$ holds everywhere, precluding the asymmetry seen in Figure 1. This example illustrates only one simple nonlinear phenomenon that can occur even with well-recorded events, 1-D Earth models, and Gaussian data errors (our computations used a Gaussian error model).

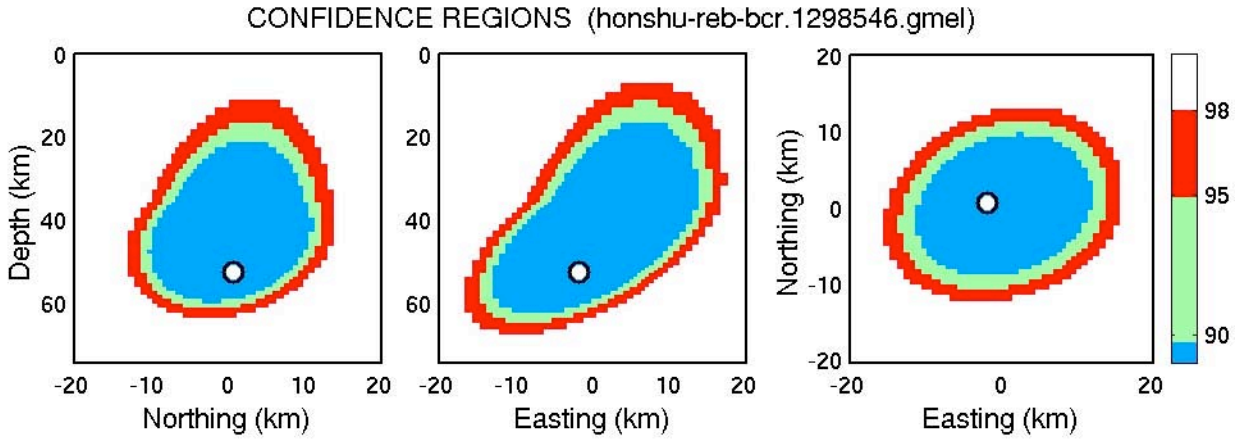


**Figure 1: Confidence regions for a 1998 earthquake in Honshu determined using 23 REB arrival time data (2 Pn, 1 Sn, 18 P, 1 S and 1 PKP). Confidence regions at three confidence levels are displayed: 90% (inner (blue) shaded area), 95% (combined inner and central (blue and green) shaded areas), and 98% (inner, central and outer (blue, green and red) shaded areas). *Left and middle frames*: cross-sections through 3-D confidence regions on the event hypocenter. *Right frame*: 2-D confidence regions on the event epicenter. The circle marks the event location reported in the REB.**

A second example of Monte Carlo confidence regions is shown in Figure 2. These are for an event (no. 91135030) from the 1991 Racha, Georgia earthquake sequence, studied by Myers and Schultz (2000). The data set comprised P wave arrival times from six stations, obtained from ISC and supplemented with picks made by F. Ryall of LLNL. The stations cover an epicentral distance range of 6° to 22°.

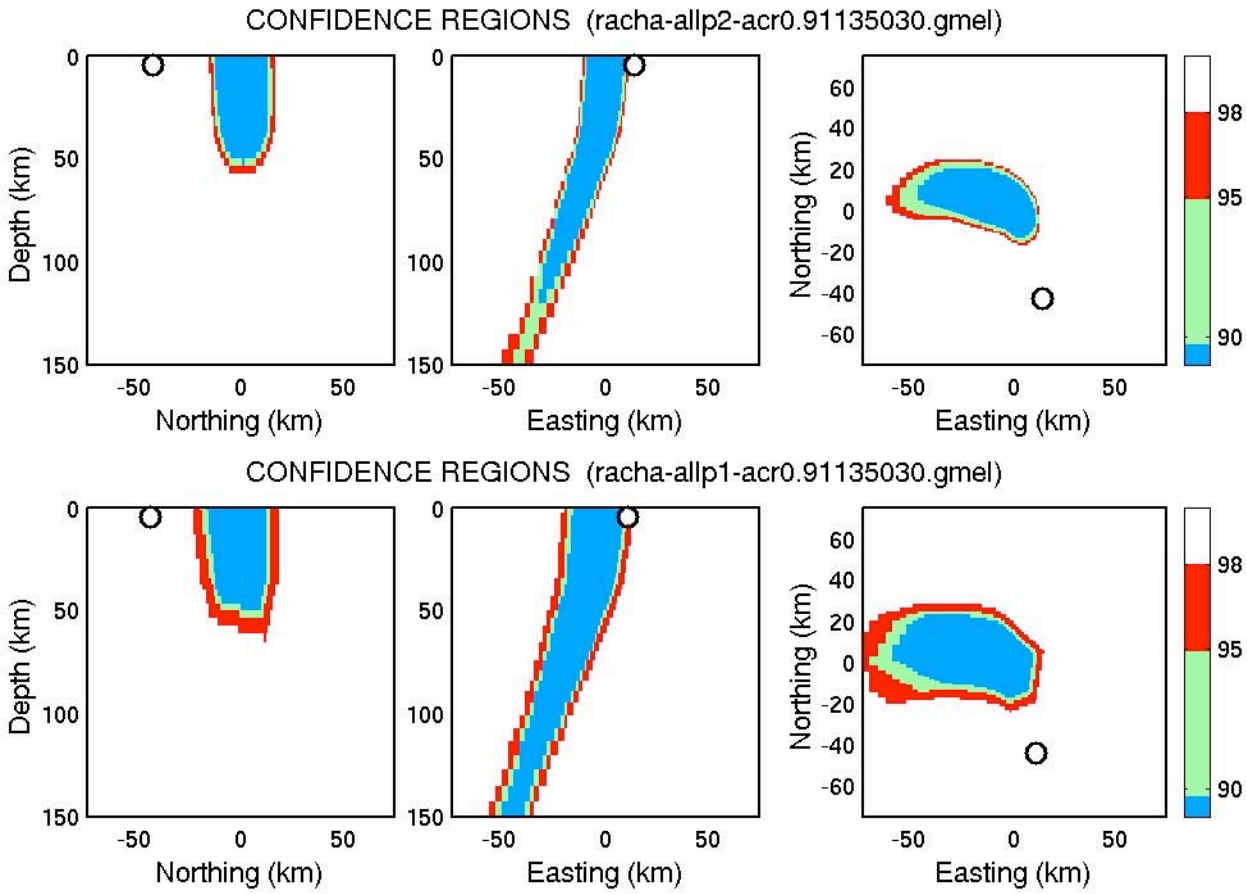


**Figure 2: Confidence regions (at 90, 95 and 98%) for an event from the 1991 Racha earthquake sequence. The data set used comprised first-arrival P wave times at six regional stations, with epicentral distances varying from 6 to 22°. The top frames are based on the assumption of Gaussian picking errors ($p$ = 2). The bottom frames assume the errors are from a Laplace (two-sided exponential) ($p$ = 1). *Left and middle*: Cross-sections of 3-D confidence regions on the event hypocenter, taken through the maximum-likelihood location. *Right*: Confidence regions on epicenter. The circle in each plot marks the local network location for the event reported by Myers and Schultz (2000). The maximum-likelihood epicenter is at zero northing and zero easting.**

We computed confidence regions using two different assumptions about the probability distribution of picking errors. The top frames of Figure 2 assumed a Gaussian distribution ($p$ = 2) while the bottom frames assumed a Laplace distribution ($p$ = 1). Even in the Gaussian case we see that the confidence regions are blatantly non-elliptical, especially the epicentral confidence regions (rightmost frames). As with the Honshu events, a big contributor to non-ellipticity is the nonlinearity of the travel-times with respect to event depth. This factor is even more significant in this example because the event depth is so poorly constrained by the sparse network available. We also see that Laplace-error confidence regions (bottom frames of Figure 2) are blockier and larger than Gaussian-error ones, which can be attributed to the differing properties of $L_1$ and $L_2$ error norms.

We note that the confidence regions in Figure 2 do not cover the GT location inferred by Myers and Schultz (the circles in each frame), and our maximum-likelihood location is biased by about 30 km. This is because we did not apply travel-time corrections to the data, or attempt to account for them as modeling errors in the computation of the confidence regions.

**Multiple-Event Location Confidence Regions**

Our multiple-event location algorithm (GMEL) solves jointly for the location parameters, $x_i$ and $t_i$, of $m$ events, and the travel-time correction terms, $a_j$, for $n$ stations. It finds maximum-likelihood solutions for these unknown parameters, using the multiple-event, multiple-station version of the likelihood function in equation (5) Like its single-event predecessor, GMEL implements the generalized Gaussian error model, this time allowing unknown station-specific scale factors, $\gamma_j$, on the standard errors, i.e.

$$\sigma_{ij} = \gamma_j \omega_{ij} \tag{11}$$

where the $\omega_{ij}$ are specified weights. Hard bounds on all the unknown parameters, including upper and lower bounds on the $a_j$, are allowed. GMEL finds the maximum-likelihood solutions for the parameters by iterating over alternating loops over events, to update event locations with station terms fixed, and over stations, to update the station terms and station scale factors, with the event locations fixed. Grid-search is used to find the optimal event locations (see Rodi et al., 2002).

To define confidence regions on one of the $m$ events in the multiple-event location problem, we have adapted our location uncertainty approach as follows. Let us denote the likelihood function for the multiple-event location problem as $L(\mathbf{x}_1, t_1, \mathbf{x}_2, t_2, \ldots, \mathbf{x}_m, t_m, a_1, \gamma_1, a_2, \gamma_2 \ldots, a_n, \gamma_n; \mathbf{d})$, where the vector $\mathbf{d}$ now contains the data for all events and stations. Let us arbitrarily identify the event of interest to be the first ($i$ =1). To define a confidence region on its hypocenter, $\mathbf{x}_1$, our uncertainty paradigm tells us to define a test-statistic, $\Gamma(\mathbf{x}_1, \mathbf{d})$ that compares two values of the likelihood function. The first is the value achieved by maximizing $L$ over all event and station parameters: $\mathbf{x}_1, t_1, \mathbf{x}_2, t_2, \ldots, \mathbf{x}_m, t_m$ and $a_1, \gamma_1, a_2, \gamma_2, \ldots, a_n, \gamma_n$. The second value of $L$ is that achieved by maximizing $L$ over all the parameters except $\mathbf{x}_1$, which is held fixed. Maximization of $L$ in both cases is performed subject to available GT constraints on any of the event locations. We will not write the formula for $\Gamma(\mathbf{x}_1, \mathbf{d})$ but it is analogous to equation (9).

Given this, our method for computing a confidence region on $\mathbf{x}_1$ is a two-step process analogous to the single-event case:

1. Sample $\Gamma(\mathbf{x}_1, \mathbf{d})$ for values of $\mathbf{x}_1$ on a dense grid.

2. Compute Monte Carlo realizations of $\Gamma(\mathbf{x}_1^{tru}, \mathbf{d}^{syn})$ for many random realizations of (multiple-event) synthetic data, $\mathbf{d}^{syn}$.

Each computation of $\Gamma$, whether for real or synthetic data, now entails computing the solution to a multiple-event inverse problem involving the data and parameters for all events and stations.

This approach to location confidence regions implicitly accounts for the uncertainty in $\mathbf{x}_1$ induced by its trade-off with the travel-time corrections, $a_j$, as they are constrained by the multiple-event data set and GT information on the other events. It avoids the need for an explicit uncertainty model for the station terms, which would then be treated as modeling errors added to the picking errors. This implicit approach takes into account correlations and the finite accuracy of GT events, and handles nonlinearity and non-Gaussian data errors.

**Example from the Izmit Earthquake Sequence**

We show some preliminary results of our multiple-event uncertainty approach applied to the 17 August 1999 Izmit, Turkey, earthquake and 32 of its aftershocks. The data set contains approximately 3500 Pn and teleseismic P arrival times from 640 stations from National Earthquake Information Center (NEIC), which we obtained courtesy of R. Engdahl and the IASPEI Working Group on Multiple-Event Location. Previously, Engdahl and Bergman (2001) applied the hypocentroidal decomposition (HDC) method to this cluster and a similar cluster from the 12 November 1999 Duzce earthquake sequence. We show confidence regions that we have computed for one of the events in the Izmit cluster.

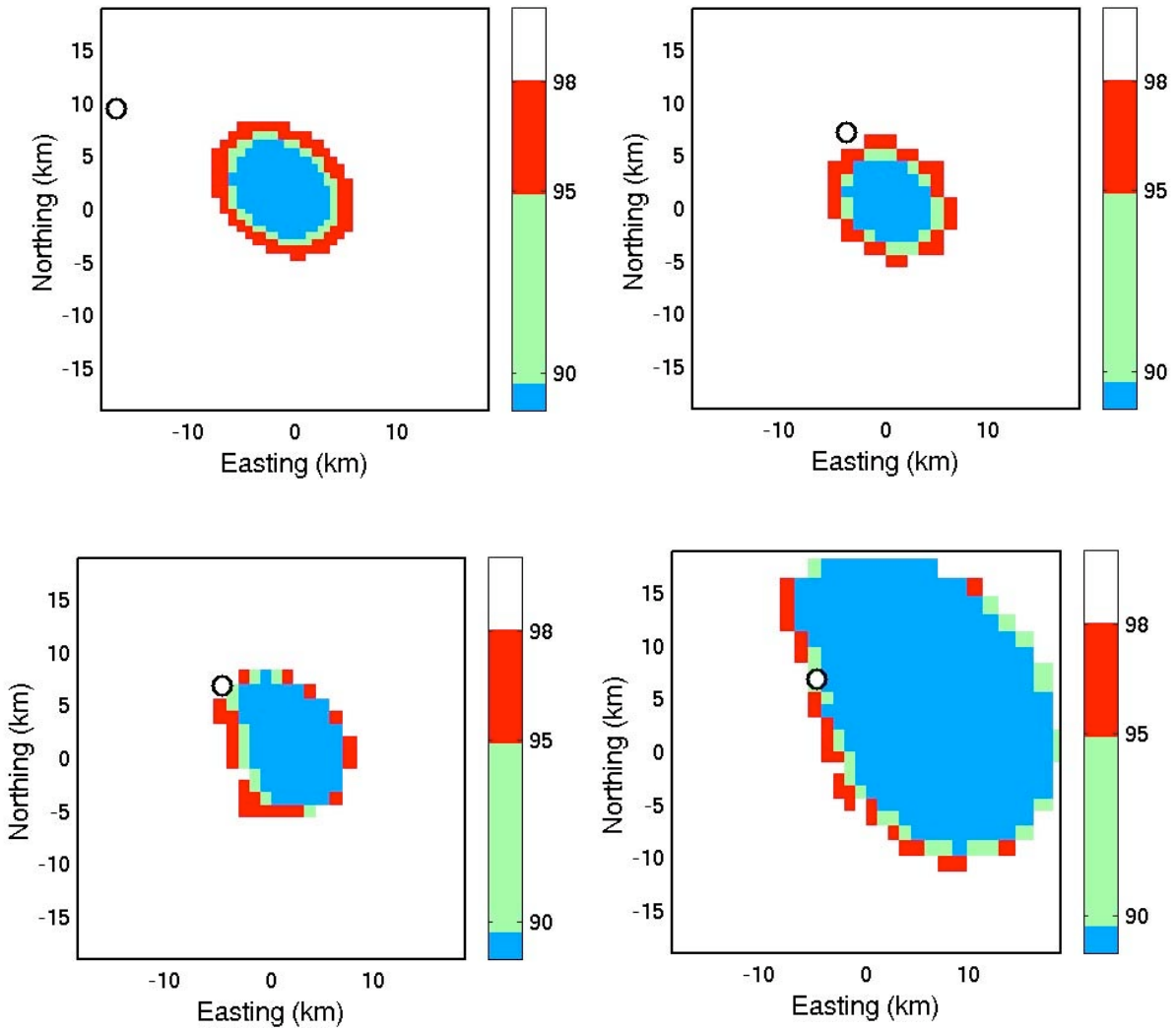


**Figure 3:** ***Top left*****: Single-event epicentral confidence regions (at 90, 95 and 98% confidence) for a well-recorded aftershock of the 1999 Izmit, Turkey earthquake. Station travel-time corrections were assumed to be zero.** ***Top right and bottom*****: Multiple-event confidence regions for the same event.** ***Top right*****: computed with the Izmit mainshock constrained as a GT0 event.** ***Bottom left*****: computed with the Izmit mainshock constrained as a GT5 event.** ***Bottom right*****: computed using no GT constraints on any events. In each frame, the circle marks the ground-truth (GT5) epicenter for the aftershock.**

The event we consider is a well-recorded aftershock occurring on 31 August 1999, and has 138 defining phases in the data set (compared to 388 defining phases for the Izmit mainshock). The top/left frame of Figure 3 shows the single-event, epicentral confidence region for this event, computed independently of the other events and with zero travel-time corrections at the stations ($a_j = 0$). Gaussian data errors were assumed and the depth of the event was fixed. The circle marks a GT5 location for the aftershock determined from a local seismic network (provided by R. Engdahl for the IASPEI Working Group). We see that the single-event confidence region is displaced by about 20 km from the GT location, and even the 98% confidence region does not include the GT location. This is expected since travel-time corrections were not applied to the AK135 travel-time tables that were used in the computations.

The other frames of Figure 3 show different versions of multiple-event confidence regions for the same Izmit aftershock. In each case, the event was located jointly with the 32 other events and the estimation of travel-time corrections at the roughly 640 stations in the data set. These other 32 events, which include the Izmit mainshock, play the role of calibration events. The different versions of multiple-event confidence regions have to do with

different GT constraints we used for the calibration events. The top/right frame assumed that the Izmit mainshock is a GT0 event. Thus, the mainshock was constrained to its local network solution while the other event epicenters were free to vary. The bottom/left frame also assumed the Izmit mainshock was the only GT event, but this time it was assumed to be GT5, i.e. its epicenter was constrained to be within 5 km of the local network solution. The bottom/right frame uses no GT constraints on any of the events. In each frame, the maximum-likelihood solution for the aftershock found by GMEL is in the center of the plot (at zero northing and easting) although it is not marked. In the top/right frame this is near the center of the confidence region, but this is not the case for the bottom two frames.

Comparing the top frames of Figure 3, we see that the multiple-event confidence region for the aftershock is much closer to its local network solution than was the case for the single-event confidence region. This is because the requirement that the event locations of all the events be self-consistent with the station travel-time corrections, combined with the GT0 constraint on the mainshock, removes much of the bias in the GMEL location that we saw in the single-event case. However, the local network solution (which might be in error by as much as 5 km) is a little outside the confidence regions at each confidence level. In the bottom/left frame, which assumed the mainshock was GT5, the confidence region for the aftershock is slightly larger, as expected, and comes closer to including the local network solution. In the bottom/right frame, we see that the multiple-event confidence region resulting from no GT constraints is much larger. This largely reflects the fact that, in small-aperture multiple-event location, there is a strong trade-off between the centroid of the cluster and the station corrections; i.e. absolute events locations cannot be determined without GT constraints. In the linear theory (Jordan and Sverdrup, 1981) this indeterminacy is total, and yet the confidence region in the bottom/right frame is finite. The probable explanation for this is that, for computational reasons, we limited the extent to which event locations could trade off with station travel-time corrections to 15 km. However, another reason might be that we imposed hard bounds on the station travel-time corrections, ±10 sec relative to AK135 times, which is a reasonable assumption. It may be that this constraint also has limited the size of the confidence regions in the bottom/right frame, and may also explain why they are not centered on the ones computed *with* a GT constraint on the mainshock.

These results, while preliminary, seem to support the validity of our implicit approach to modeling errors. Further, the results suggest the possibility that, even in this simplest of joint location/calibration problems, prior constraints on both reference event locations and travel-time discrepancies from global 1-D models might be an important element in location error assessment.

## CONCLUSIONS AND RECOMMENDATIONS

We have developed a general theoretical and computational framework for characterizing the uncertainty in seismic event locations in the context of the joint inverse problem of multiple-event location and travel-time calibration. Like our earlier work on single-event location, our approach accommodates Gaussian and non-Gaussian assumptions about the picking errors in seismic arrival times, and avoids linearization of the forward travel-time problem. The most important new element of our approach is that it takes implicit account of the errors in travel-time forward models. This avoids a difficult task when the calibration and location problems are addressed separately, i.e. determining realistic uncertainty estimates in seismic calibration parameters, and then incorporating them into a single-event event location algorithm. However, our approach introduces a new difficulty in the fact that it is computationally intensive. We are investigating computational short cuts that will make our method more practical. Further, we are looking at how best to implement the approach with more general parameterizations of path corrections, including travel-time correction surfaces, so that the method is not restricted to small event clusters.

## REFERENCES

Billings, S.D., M.S. Sambridge and B.L.N. Kennett, 1994. Errors in hypocenter location: picking, model and magnitude dependence, *Bull. Seism. Soc. Am., 84,* 1978–1990.

Engdahl, E.R. and E.A. Bergman, 2001, Validation and generation of reference events by cluster analysis, *Proceedings, 23rd Seismic Research Review: Worldwide Monitoring of Nuclear Explosions*, Jackson Hole, Wyoming.

Evernden, J.F., 1969. Precision of epicenters obtained by small numbers of worldwide stations, *Bull. Seism. Soc. Am., 59*, 1365–1398.

Flinn, E.A., 1965, Confidence regions and error determinations for seismic event location, *Rev. Geophys., 3*, 157–185.

Jordan, T.H. and K.A. Sverdrup, 1981, Teleseismic location techniques and their application to earthquake clusters in the south-central Pacific, *Bull. Seism. Soc. Am., 71*, 1105–1130.

Myers, S.C., and C.A. Schultz, 2000, Improving sparse network seismic locations with Bayesian kriging and teleseismically constrained calibration events, *Bull. Seism. Soc. Am., 90*, 199–211.

Rodi, W., E.R. Engdahl, E.A. Bergman, F. Waldhauser, G.L. Pavlis, H. Israelsson, J.W. Dewey and M.N. Toksöz, 2002, A new grid-search multiple-event location algorithm and a comparison of methods, *Proceedings, 24th Seismic Research Review - Nuclear Explosion Monitoring: Innovation and Integration*, Ponte Vedra Beach, Florida, 403–411.

Rodi, W., S.C. Myers and C.A. Schultz, 2003, Grid-search location methods for ground-truth collection from local and regional seismic networks, *Proceedings, 25th Seismic Research Review Nuclear Explosion Monitoring: Building the Knowledge Base*, Tucson, Arizona (this volume).

Rodi, W., and M.N. Toksöz, 2000, Grid-search techniques for seismic event location, *Proceedings, 22nd Annual DoD/DOE Seismic Research Symposium: Planning for Verification of and Compliance with the Comprehensive Nuclear-Test-Ban Treaty (CTBT)*, New Orleans, Defense Threat Reduction Agency (DTRA).

Rodi, W., and M.N. Toksöz, 2001, Uncertainty analysis in seismic event location, *Proceedings, Proceedings, 23rd Seismic Research Review: Worldwide Monitoring of Nuclear Explosions*, Jackson Hole, Wyoming.

Sambridge, M., 1999. Geophysical inversion with a neighborhood algorithm—1. Searching a parameter space, *Geophys. J. Int., 138*, 479–494.

Schultz, C.A., S.C. Myers, J. Hipp and C.J. Young, 1998, Nonstationary Bayesian kriging: a predictive technique to generate spatial corrections for seismic detection, location, and identification, *Bull. Seism. Soc. Am., 88*, 1275–1288.